

Simulation of Unsteady Flows Through Stator and Rotor Blades
of a Gas Turbine Using the Chimera Method

S. Nakamura[†] and J. N. Scott^{††}

[†]Mechanical Engineering Department

^{††}Aeronautical and Astronautical Engineering Department
The Ohio State University
Columbus, Ohio 43210, USA

Abstract

A two-dimensional model to solve compressible Navier-Stokes equations for the flow through stator and rotor blades of a turbine is developed. The flow domains for the stator and rotor blades are coupled by the Chimera method that makes grid generation easy and enhances accuracy because the area of the grid that have high turning of grid lines or high skewness can be eliminated from the computational domain after the grids are generated. The results of flow computations show various important features of unsteady flows including the acoustic waves interacting with boundary layers, Karman vortex shedding from the trailing edge of the stator blades, pulsating incoming flow to a rotor blade from passing stator blades, and flow separation from both suction and pressure sides of the rotor blades.

1. Introduction

Most of computer codes currently used to simulate aerodynamics in compressors and turbines are based on the steady basis with a turbulence model. However these time-averaged steady-state approaches are limited in their capabilities to compute some of the most critical features encountered in turbomachinery. Among their most serious shortcomings are their inability to predict phenomena associated with unsteady nature of the flows, and their inability to accurately simulate heat transfer. This is particularly evident when computing flow through a stator and rotor combination. Because of the non-uniform flow velocities from the stator exit plane, the moving rotor blades always encounter a time-varying, or pulsating, inlet flow. This constantly changing flow distribution of the inlet flow causes deviations from the steady inflow and changes the flow characteristics in the rotor blade passage. The importance of simulation of unsteady flows in the rotor blade passages has been recognized as a critical capability for performance analysis and design.

The development of a code to analyze the three-dimensional transient flow through a stator and rotor is a difficult task for various reasons. To analyze the flow through a stator and rotor blades, it is necessary to include at least 5 to 6 blades in the computations because of differences in the blade pitches between the rotor and stator blades. The rotor blades are constantly moving relative to the stator blades. The computation takes significantly more cpu time not only because of the large number of blades to be considered but also because of the unsteady flow simulation. The development of more advanced codes requires both new mathematical methods for numerical computations and significantly more powerful computer resources.

The present study [1] was initiated with the background thus stated. Two major objectives of the study are, first, (a) to examine some numerical methods suitable for the flow through stator and rotor rows, and second, (b) to analyze the effect of unsteady flow from the stator to the rotor. The present work is performed using a two-dimensional model. However, the experience and results of the investigation will be useful in developing three-dimensional models.

The remainder of this paper describes a computational model for the transient flow through stator and rotor blades based on the two-dimensional compressible Navier-Stokes equations and shows results of flow computations. We assume the pitch of stator blades is identical to that of the rotor blade. Therefore, only one stator blade that is stationary and one rotor that moves linearly to the negative direction of the y-coordinate are considered in the computations. For the direction tangential to the rotor movement, periodic boundary conditions are used for both rotor and stator flow channels. The body-fitted grids are used in both stator and rotor regions, but the grid for the rotor region moves with the rotor blade. The compressible Navier-Stokes equations are solved in each domain, and coupled to each other by the Chimera method[2].

2. Basic Equations and the Solution Methods

The compressible Navier-Stokes equation for the stator domain is written as

$$Q_t + E_x + F_y = R_x + S_y \quad (1)$$

where

$$Q = \begin{bmatrix} \rho \\ \rho u \\ \rho v \\ e \end{bmatrix}, \quad E = \begin{bmatrix} \rho u \\ \rho u^2 + p \\ \rho uv \\ u(e+p) \end{bmatrix}, \quad F = \begin{bmatrix} \rho v \\ \rho uv \\ \rho v^2 + p \\ v(e+p) \end{bmatrix}, \quad R = \begin{bmatrix} 0 \\ \tau_{xx} \\ \tau_{xy} \\ \tau \end{bmatrix}, \quad S = \begin{bmatrix} 0 \\ \tau_{xy} \\ \tau_{yy} \\ s \end{bmatrix} \quad (2)$$

with

$$\begin{aligned} \tau_{xx} &= [(\lambda + 2\mu)u_x + \lambda v_y]/Re \\ \tau_{xy} &= \mu(u_y + v_x)/Re \\ \tau_{yy} &= [(\lambda + 2\mu)v_y + \lambda u_x]/Re \end{aligned} \quad (3)$$

$$\tau = u\tau_{xx} + v\tau_{xy} + \beta(a^2)_x$$

$$s = u\tau_{xy} + v\tau_{yy} + \beta(a^2)_y$$

Here, ρ is the density, u and v are the velocity components, p is the pressure, e is the total energy, and all the variables are non-dimensionalized by

$$\begin{aligned} x &= \bar{x}/\bar{L}, \quad y = \bar{y}/\bar{L} \\ \rho &= \bar{\rho}/\bar{\rho}_o, \quad u = \bar{u}/\bar{a}_o, \quad v = \bar{v}/\bar{a}_o \\ p &= \bar{p}/(\bar{\rho}_o \bar{a}_o), \quad e = \bar{e}/(\bar{\rho}_o \bar{a}_o) \\ \mu &= \bar{\mu}/\bar{\mu}_o, \quad \lambda = \bar{\lambda}/\bar{\lambda}_o \end{aligned} \quad (4)$$

$$t = \bar{a}_0 \bar{L}, \quad Re = \bar{\rho}_0 \bar{a}_0 L / \bar{\mu}_0$$

Here the quantities with an overbar is the dimensional quantity, and those with subscript o is the value at the inlet. The variables x and y are coordinates, L is a reference length, μ and λ are viscosities, a is the sound speed. The pressure is related to the conservative flow variables by

$$p = (\gamma - 1) \left(e - \frac{1}{2} \rho (u^2 + v^2) \right) \quad (5)$$

For the rotor domain that moves with the rotor blade, Eq.(1) holds but the variables are redefined by

$$Q = \begin{bmatrix} \tilde{\rho} \\ \tilde{\rho} \tilde{u} \\ \tilde{\rho} \tilde{v} \\ \tilde{e} \end{bmatrix}, \quad E = \begin{bmatrix} \tilde{\rho} \tilde{u} \\ \tilde{\rho} \tilde{u}^2 + \tilde{p} \\ \tilde{\rho} \tilde{u} \tilde{v} \\ \tilde{u}(\tilde{e} + \tilde{p}) \end{bmatrix}, \quad F = \begin{bmatrix} \tilde{\rho} \tilde{v} \\ \tilde{\rho} \tilde{u} \tilde{v} \\ \tilde{\rho} \tilde{v}^2 + \tilde{p} \\ \tilde{v}(\tilde{e} + \tilde{p}) \end{bmatrix}, \quad R = \begin{bmatrix} 0 \\ \tilde{\tau}_{xx} \\ \tilde{\tau}_{xy} \\ \tilde{r} \end{bmatrix}, \quad S = \begin{bmatrix} 0 \\ \tilde{\tau}_{xy} \\ \tilde{\tau}_{yy} \\ \tilde{s} \end{bmatrix} \quad (6)$$

$$\tilde{\tau}_{xx} = [(\lambda + 2\mu)\tilde{u}_x + \lambda\tilde{v}_y]/Re$$

$$\tilde{\tau}_{xy} = \mu(\tilde{u}_y + \tilde{v}_x)/Re \quad (7)$$

$$\tilde{\tau}_{yy} = [(\lambda + 2\mu)\tilde{v}_y + \lambda\tilde{u}_x]/Re$$

$$\tilde{s} = \tilde{u}\tilde{\tau}_{xy} + \tilde{v}\tilde{\tau}_{yy} + \beta(\tilde{a}^2)_y$$

The pressure is related to the conservative flow variables by

$$\tilde{p} = (\gamma - 1) \left(\tilde{e} - \frac{1}{2} \tilde{\rho} (\tilde{u}^2 + \tilde{v}^2) \right) \quad (8)$$

Other nondimensional variables are

$$\tilde{x} = \bar{x}/\bar{L}, \quad \tilde{y} = \bar{y}/\bar{L}$$

$$\tilde{\rho} = \bar{\rho}/\bar{\rho}_0, \quad \tilde{u} = \bar{u}/\bar{a}_0, \quad \tilde{v} = \bar{v}/\bar{a}_0$$

$$\tilde{p} = \bar{p}/(\bar{\rho}_0 \bar{a}_0), \quad \tilde{e} = \bar{e}/(\bar{\rho}_0 \bar{a}_0)$$

$$\mu = \bar{\mu}/\bar{\mu}_0, \quad \lambda = \bar{\lambda}/\bar{\lambda}_0$$

and t and Re are common for the two domains.

$$t = \bar{a}_0 \bar{L}, \quad Re = \bar{\rho}_0 \bar{a}_0 L / \bar{\mu}_0 \quad (9)$$

At the interface between the stator region and the rotor region, the relations between the

variables are

$$\tilde{u} = u, \quad \tilde{v} = v - \tilde{V}, \quad \tilde{\rho} = \rho, \quad \tilde{p} = p \quad (10)$$

where \tilde{V} is the nondimensional velocity of the rotor given by

$$\tilde{V} = \tilde{\omega} r/a_0$$

Introducing Eq.(4) and Eq.(8) into

$$\tilde{p} = p$$

yields

$$e - \frac{1}{2}\rho(u^2 + v^2) = \tilde{e} - \frac{1}{2}\tilde{\rho}(\tilde{u}^2 + \tilde{v}^2)$$

or equivalently

$$\tilde{e} = e - \frac{1}{2}\rho[v^2 - (v - \tilde{V})^2]$$

or

$$e = \tilde{e} + \frac{1}{2}\rho[(\tilde{v} + \tilde{V})^2 - \tilde{v}^2] \quad (11)$$

3. Computational Procedure

The Navier-Stokes equations are transformed onto a rectangular computational domain, and solved by the implicit method based on the LU decomposition [4]. The Navier-Stokes code is based on the second-order accurate implicit method. However, the boundary condition along the trailing cut and the Chimera coupling both use the computed results from the previous time step. Therefore, the accuracy of the whole solution reduces to the first order in time at least locally. The grid for each region is generated independently by the elliptic-hyperbolic method[3]. Two grid systems are used, one 38x220 points per blade, and another 55x658 points per blade. The grid points along the trailing cut in the grid are not made continuous across the cut because otherwise very high skewness of grid occurs under the periodicity constraints of the grid.

The inflow boundary conditions for the rotor domain are taken from the most updated computational results for the stator domain by the Chimera method. At the same time, the exit boundary conditions for the stator domain are taken from the most updated computational results from the rotor flow domain. The points along the inlet for the rotor regions are not same as the left boundary of the rotor grid so the front area of the rotor grid with significant turning can be avoided. Likewise, the exist boundary for the stator domain does not coincide with the right boundary of the stator grid.

The conventional method of coupling the two domains is as follows. The grid line which is vertical at the exit of the rotor domain would match the vertical grid line at the flow entrance of the rotor grid. However, the rotor grid is moving with the rotor blades, so flow boundary conditions are exchanged between the two domains by means of one-dimensional interpolations. Since the rotor grid is constantly moving relative to the stator grid, the interpolation relations also constantly changes. With the conventional approach, the grid for the flow exit of the stator and the grid at the

entrance to the rotor should be carefully aligned. Whenever the distance between the stator and the rotor is altered, a new set of grids should be generated. Generally the grid lines in a c-grid for a turbomachinery blade have high turns at the top left and bottom left corner of the grid for a blade where the accuracy of the coordinate transformation is poor.

With the Chimera method, a code developed for a single rectangular computational domain is applied for each of the flow domain belonging to one blade. Therefore, it is not necessary to match the grid line of the exit boundary of the stator domain with the grid line of the inlet boundary of the rotor domain. With the Chimera coupling, the front area of the rotor grid with high turning of grid lines may be removed from the actively used computational domain. Likewise the rear domain of the stator where high skewness of the grid tend to occur can be removed. The Chimera coupling requires two-dimensional interpolation to exchange boundary conditions between the stator and rotor. The interpolative exchanges of the boundary conditions disturb continuity of the field values across the boundaries of the two domains, but the conventional methods have the same problem. The Chimera method may be applied not only for the blade rows, but can be easily applied when additional flow domains are involved. This feature will become attractive in three-dimensional simulation particularly when the additional flow geometries such as inlet eye, volute, and exit diffuser are included (for a radial turbine).

4. Illustration of Results

The coarser grids for the stator and rotor are shown in Figures 1, where only every other grid lines that are parallel to the blade surface are omitted for clarity. The finer grids of 55x658/blade were generated by interpolation of the coarser grids (not shown here).

Figures 2 illustrates density distribution at two different stator-rotor positions, which were developed as follows. The coarser grids of 38x220/blade were used for this flow computation. There are some overlapping between the computed flow domains for the stator and the rotor blades. The mid point in the overlapping area will be denoted by $x=A$. The density distribution is plotted for $x<A$, and the density distribution from the rotor calculation is plotted for $x>A$. Discontinuity of the density contours is due to the interpolating scheme to couple the two domains in the Chimera scheme. Note, however, that even if no smearing effect due to interpolation exists, the wake from the trailing edge of the stator blade does not go into the rotor domain, because the plotting on the rotor domain is based on the relative coordinate. The grid size in the wake region of the stator is significantly smaller than that in front of the rotor blade. The difference of the grid sizes is also responsible to the discontinuity of the contours than Chimera coupling effects.

An examination of Fig.2 reveals that shapes of density contours at these different time points, namely at different stator-rotor positions, are different. It is caused by the unsteady inlet flow to the rotor primarily because of changing relative position of the rotor to the stator blades. To show the effect of the moving relative positions, distribution of several flow quantities along a vertical line indicated in Figure 1 are plotted in Figure 3 in order of increasing time in cycle 8. The initial numerical transient of the solution such as propagation of acoustic waves disappears after two cycles. At the eighth cycle, the same time-dependent flow distribution repeats during each cycle.

The computation with the finer grid of 55x658 was performed for the same geometry and physical constants as for the computation illustrated in Figure 2 and 3. Because of a massive amount of data from the finer grid computations, we have not yet been able to analyze the results to a full extent. However, snapshots of density distribution for a few selected time steps are illustrated in Figure 4. Figure 4a is a density distribution that occurs during the initial numerical transient and shows interaction between acoustic waves and boundary layers. Although the initial numerical transient is not a true physical phenomena, the flow behavior during that period still provides important information because similar transient should occur in case a sudden change of

inlet or exit flow conditions change or the load to the turbine impulsively changes. Figure 4b is for a later time than Fig. 4a but still in a late stage of the initial numerical transient. This figure shows Karman vortex shedding from the trailing edge of the stator blade, and flow separation from the suction side of the rotor blade. Figure 4c is for a time step after the rotor blades has passed stator blades seven times. The figure shows a flow separation at the lower surface of the rotor blade and a vortex being shed. A periodic shedding of vortices from the same location has been observed. At this time of writing it is not certain, however, if this vortex shedding phenomena is simply due to periodic change of the inlet flow to the rotor blade or induced by the Karman vortices from the trailing edge of the stator. But the latter is be highly likely. Karman vortices from the trailing edge are also observed in Figure 4c (Karman vortices are more clearly shown in the next figure). Figure 4d (the number of contour lines are significantly increased to show details more clearly) shows Karman vortex street from the trailing edge of the stator blade at a different time step. Unlike the vortex shedding from a simple circular cylinder, the geometrical pattern of Karman Vortices from a turbine blade seem to be much irregular.

5. Concluding Remarks

Two dimensional modeling of the flow through stator and rotor rows based on the Chimera method has been described. The computational results show several important aspects of the unsteady flow through stator and rotor passages. The unsteady flow phenomena captured in the present computational simulation are not only interesting from academic curiosity but also worth further investigation of practical interest, particularly to understand the mechanism of heat transfer in turbomachinery.

Acknowledgements

The authors are thankful to R. V. Chima and K. C. Civinscus of NASA Lewis Research Center for providing data and comments that were very useful for the present study. The Chimera-coupled compressible Navier-Stokes code described here was developed by modification of the compressible Navier-Stokes code originally developed by S. Obayashi for a single airfoil. A part of the grid generation was performed by a computer at NASA Lewis. The flow solution was obtained on Cray YMP at Ohio Supercomputer Center. The first author also thank Ohio Aerospace Institute for their support for an initial stage of this study

References

- [1] S. Nakamura, J. N. Scott, "Computational Simulation of Unsteady Flows through Stator and Rotor Passage of a Gas Turbine," Proc. International Symposium of Experimental and Computational Aerothermodynamic of Internal Flows, Prague, Czech Republics, July 12-15, 1993
- [2] J. L. Steger, F. C. Dougherty, and J. A. Benek, "A Chimera Grid Scheme," in *Advances in Grid Generation*, ed. K. Ghia and U. Ghia, ASME FED Vol-5, 1983
- [3] S. Nakamura, M. Spradling, D. Fradl, and K. Kuwahara, "A Grid Generating System for Automobile Aerodynamic Analysis," in *Vehicle Aerodynamics: Recent Progress*, SAE SP-855, 1991
- [4] S. Obayashi, K. Kuwahara, and H. Kubota, "Computation of Unsteady Shock-Induced Vortex Separation," AIAA 85-0183, 1985

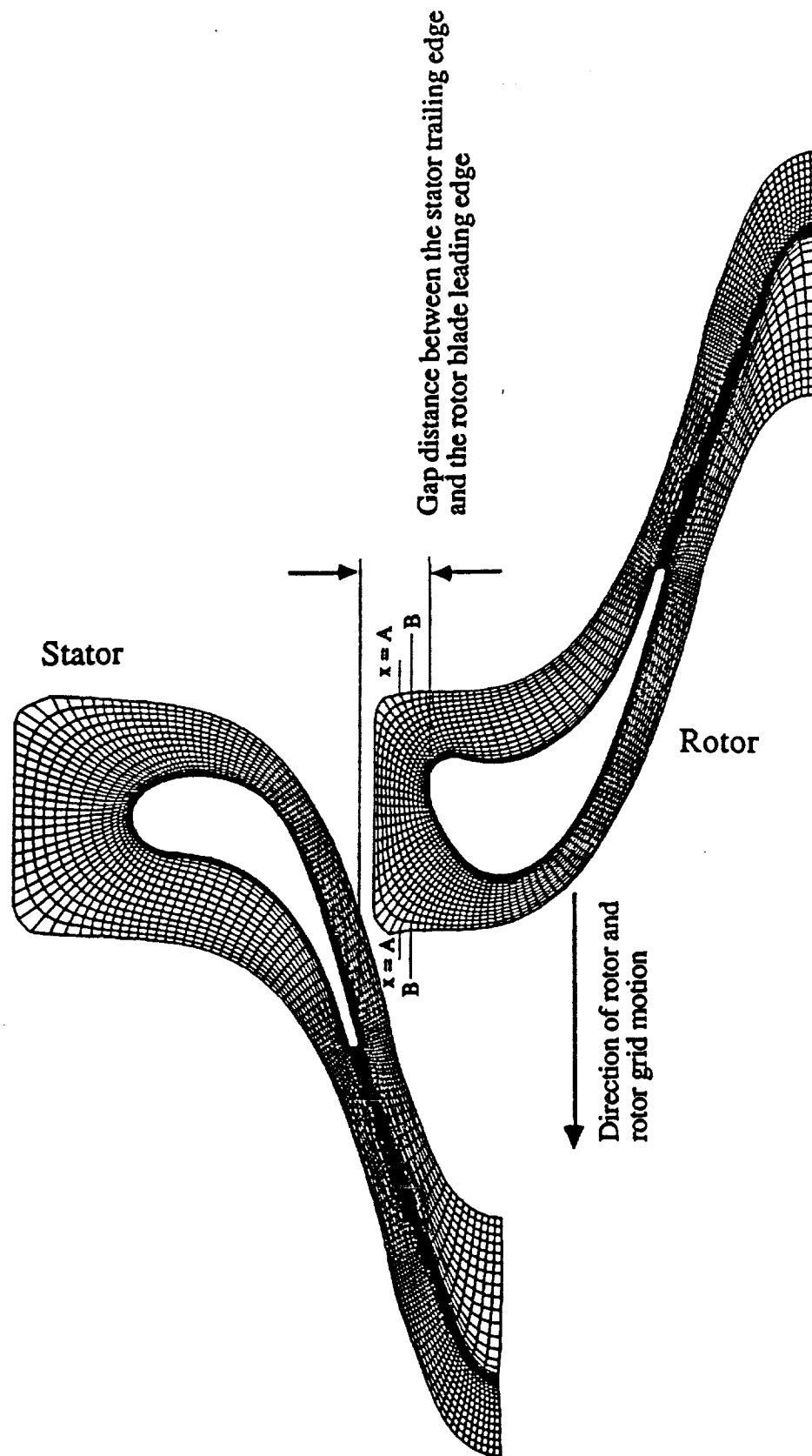


Figure 1 Grids for the stator and rotor domains (only half of the points in the directions intersecting the blades and trailing cut are plotted)

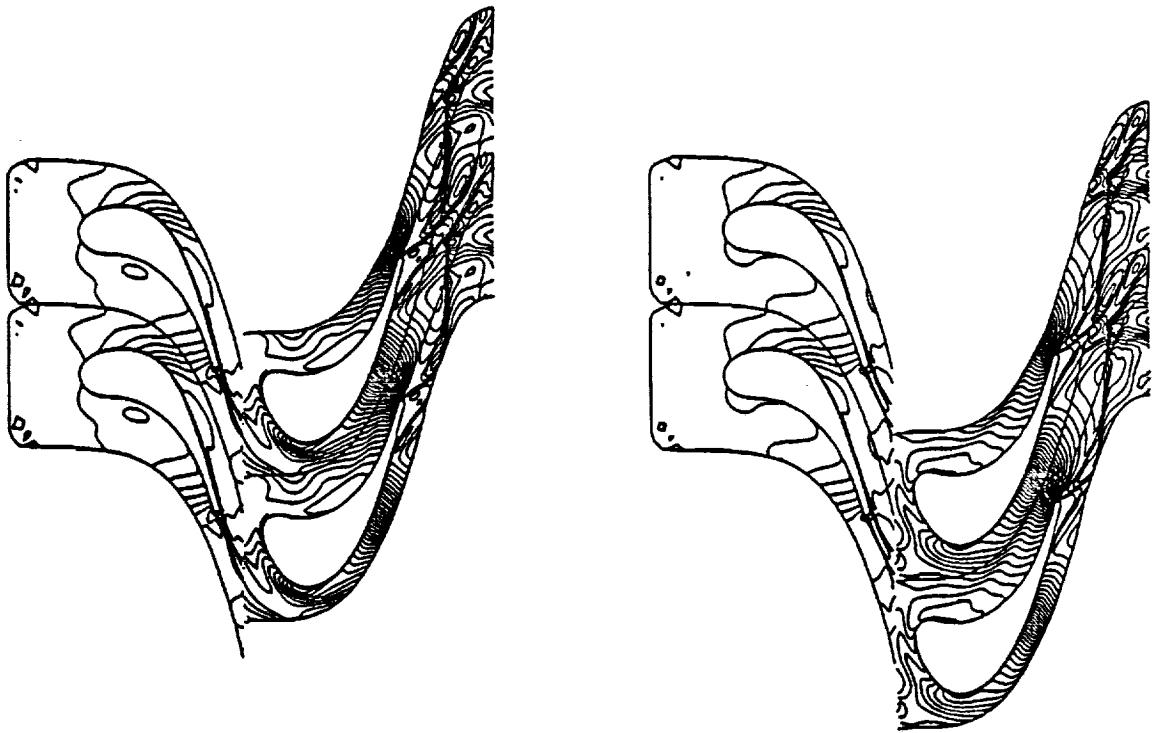


Figure 2 Density contour plot for two different positions of rotor blades relative to stator blades

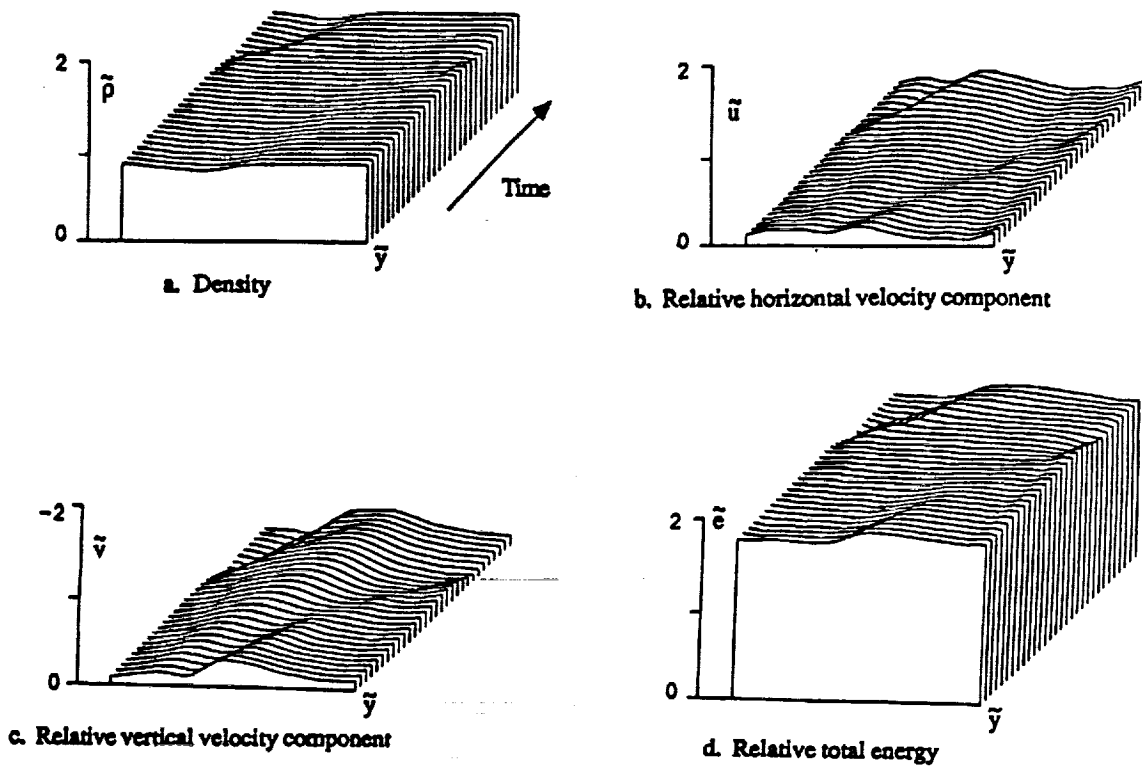
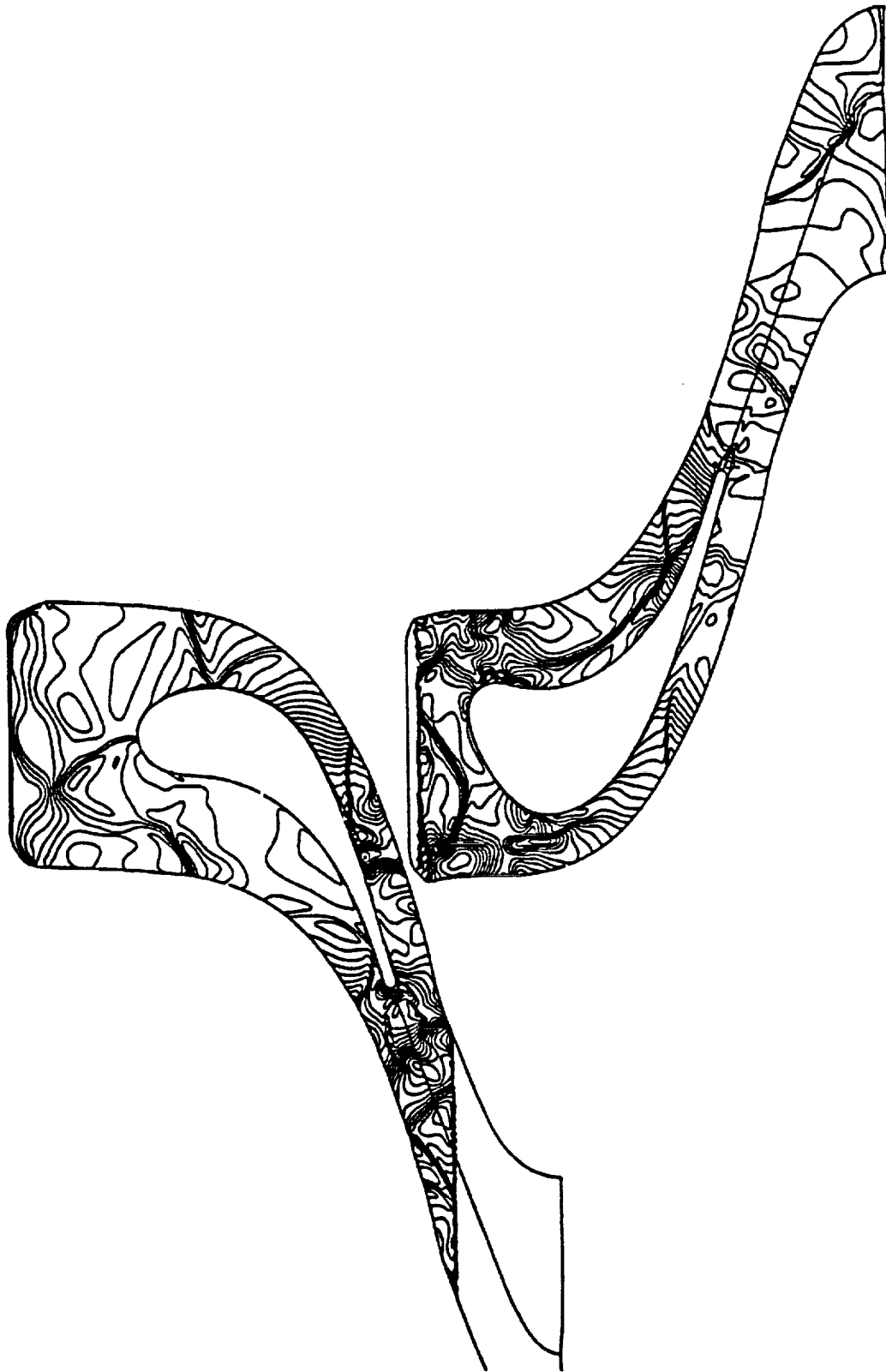
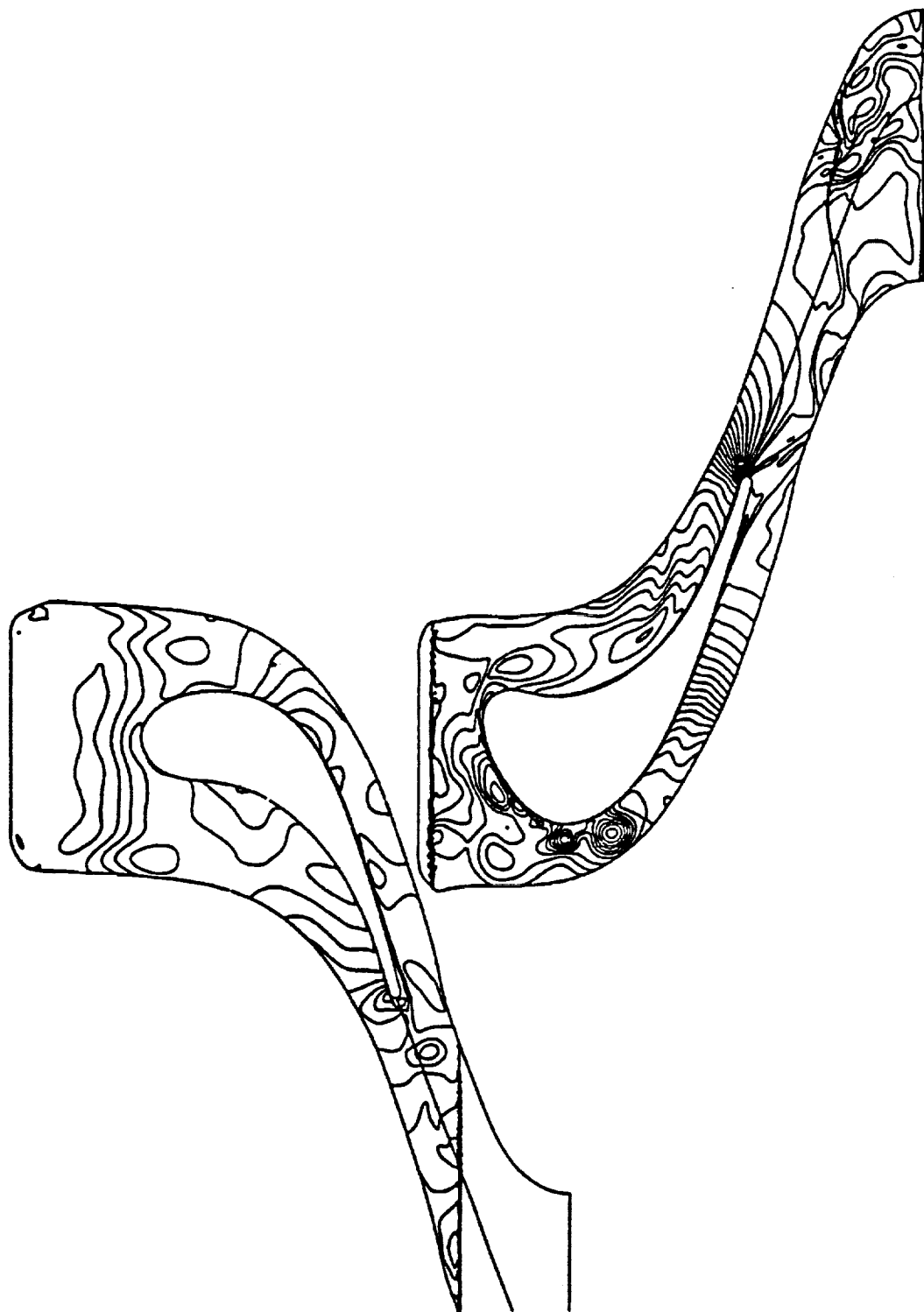


Figure 3 Time-dependent variations of spatial distributions of field variables in front of the rotor blade leading edge (see A-A line in Figure 1)



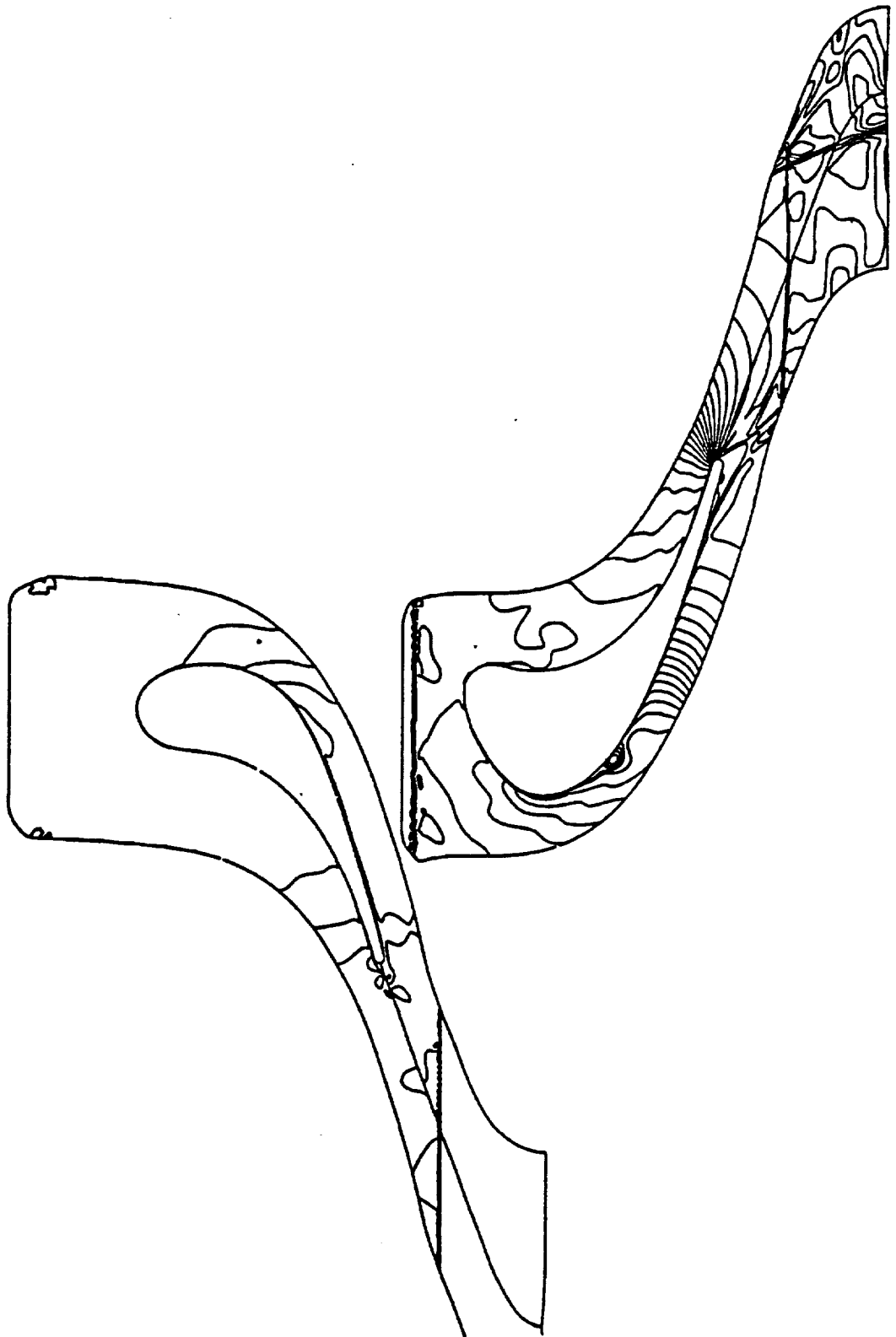
4a: during the initial numerical transient

Figure 4 Snapshots of density contours at different time steps (55x658 points/blade)



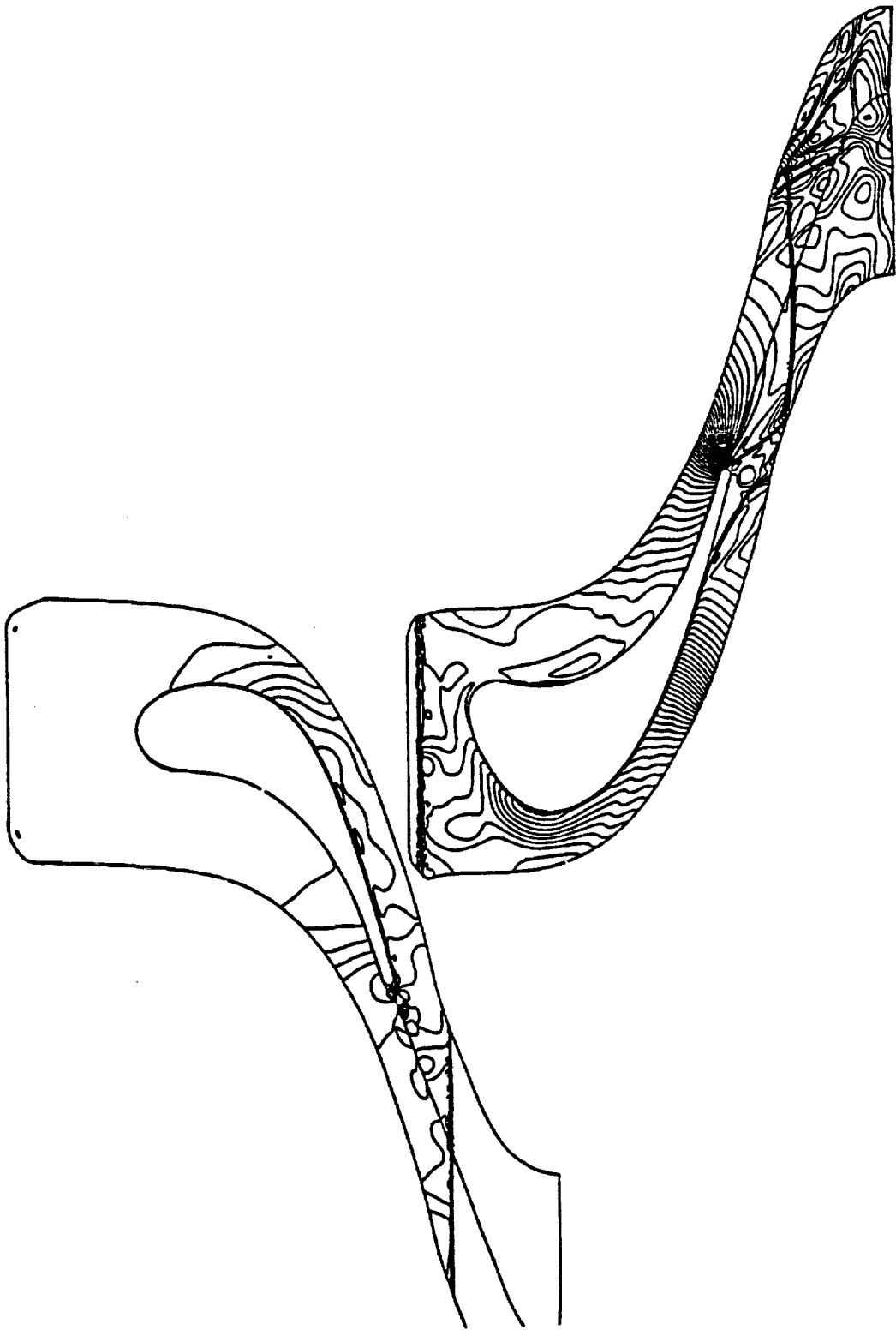
4b: a later stage of the initial numerical transient

Figure 4 continued



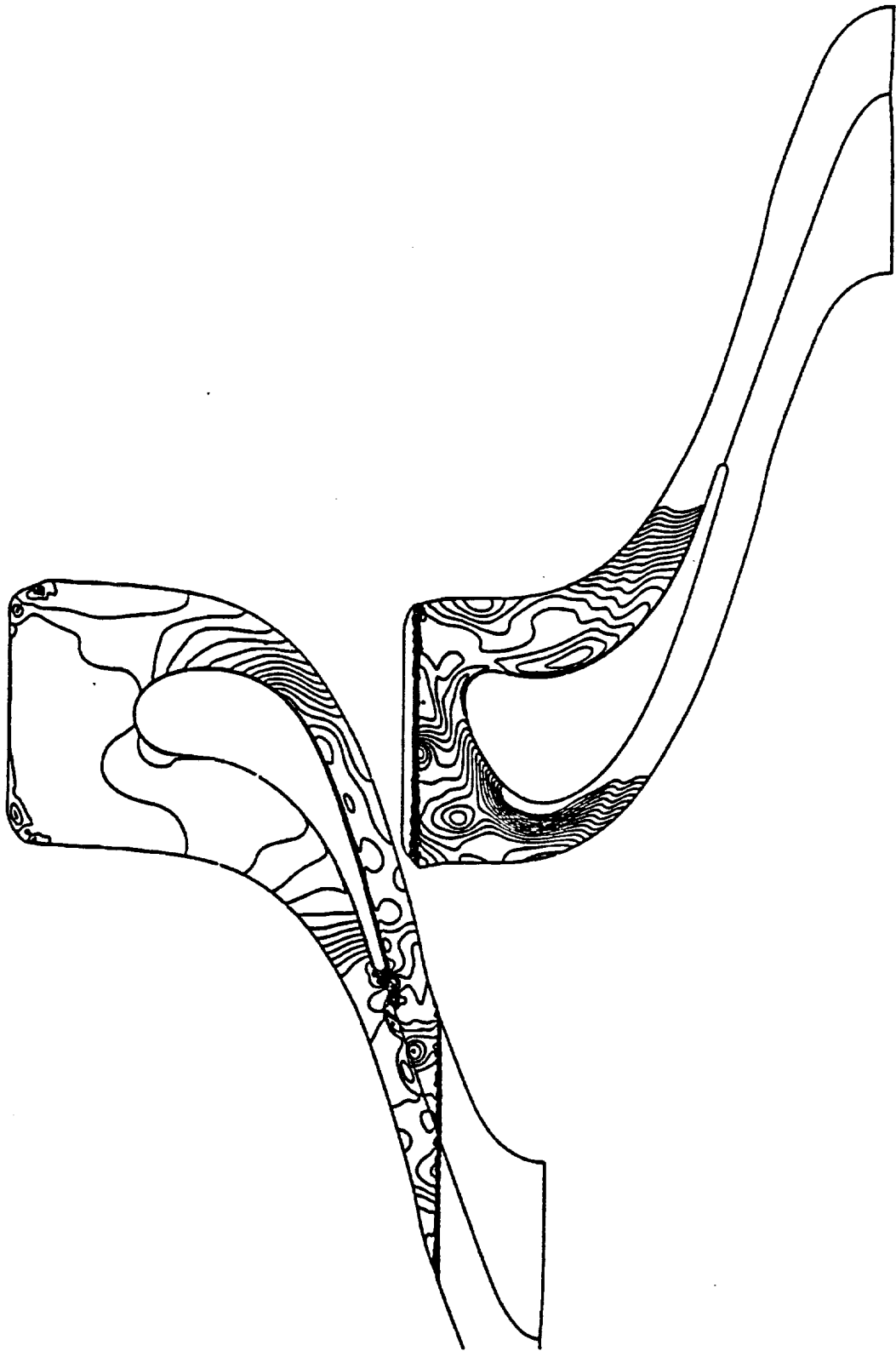
4c: a time step long after the initial numerical transient

Figure 4 continued



4d: another time step long after the initial numerical transient
(with a higher contour density than 4c)

Figure 4 continued



4d': repeat of 4d (with a much higher contour density)

Figure 4 continued

